Evidence for charge symmetry violation in parton distributions

C. Boros
Department of Physics and Mathematical Physics, and Special Research Center for the Subatomic Structure of Matter, University of Adelaide, Adelaide 5005, Australia

J. T. Londergan
Department of Physics and Nuclear Theory Center, Indiana University, Bloomington, Indiana 47405

A. W. Thomas
Department of Physics and Mathematical Physics, and Special Research Center for the Subatomic Structure of Matter, University of Adelaide, Adelaide 5005, Australia

(Received 2 October 1998; published 9 March 1999)

By comparing structure functions measured in neutrino and charged lepton deep inelastic scattering, one can test the validity of parton charge symmetry. New experiments allow us to make such tests, which set rather tight upper limits on parton charge symmetry violation (CSV) for intermediate Bjorken x, but which appear to show sizable CSV effects at small x. We show that neither nuclear shadowing nor contributions from strange and antistrange quark distributions can account for the experimentally observed difference between the two structure functions. We are therefore forced to consider the possibility of a large CSV effect in the nucleon sea quark distributions. We discuss the consequences of this effect for other observables, and we propose an experiment which could detect a large CSV component in the nucleon sea. [S0556-2821(99)03507-9]

PACS number(s): 13.60.Hb, 11.30.Hv, 12.39.Ki, 13.15.+g

I. INTRODUCTION

In discussing the strong interaction, it is customary to assume the validity of charge symmetry, which interchanges protons and neutrons (simultaneously interchanging up and down quarks). For example, all phenomenological analyses of deep inelastic scattering data in terms of parton distribution functions assume charge symmetry from the beginning. Our faith in charge symmetry is justified from our experience in nuclear physics, where this symmetry is respected to a high degree of precision. Most experimental low-energy tests of charge symmetry find that it is good to at least 1% in reaction amplitudes [1,2]. Until recently such an assumption seemed to be justified, as there was no compelling experimental evidence against parton charge symmetry. The quantitative evidence which could be extracted from high energy experiments, although not particularly precise, was consistent with charge symmetric parton distributions [3].

Experimental verification of charge symmetry is difficult, partly because the relative charge symmetry violation (CSV) effects are expected to be small, requiring high precision experiments to measure CSV effects, and partly because CSV often mixes with parton flavor symmetry violation (FSV). Recent experimental measurements by the New Muon Collaboration (NMC) [4], demonstrating the violation of the Gottfried sum rule [5], have been widely interpreted as evidence for what is termed SU(2) FSV. The measurement of the ratio of Drell-Yan cross sections in proton-deuteron and proton-proton scattering, first by the NA51 Collaboration at CERN [6] and more recently by the E866 experiment at Fermilab [7], also indicates substantial FSV. However, both of these experiments could in principle be explained by sufficiently large CSV effects [8,9], even in the limit of exact flavor symmetry. In view of these ambiguities in the interpretation of current experimental data, it would be highly desirable to have experiments which separate CSV from FSV. A few experiments have been already proposed [10,11] and could be carried out in the near future.

Recent experiments now allow us for the first time to make precision tests which could put tight upper limits on parton CSV contributions. The NMC measurements of muon deep inelastic scattering (DIS) on deuterium [12] provide values for the charged lepton structure function $F_2^{\mu}(x,Q^2)$. In a similar Q^2 regime the CCFR Collaboration [13] extract the structure functions $F_2^{\nu}(x,Q^2)$ from neutrino-induced charge-changing reactions. As we show in Sec. II, the ''charge ratio,'' which can be constructed from these two quantities (plus information about the strange quark distribution) can in principle place strong constraints on parton CSV distributions. We will show that, for intermediate values $0.1 \leqslant x \leqslant 0.4$, the agreement between the two structure functions is impressive, and provides the best upper limit to date on parton CSV terms. However, the charge ratio shows a substantial deviation from unity in the region $x < 0.1$, which might suggest surprisingly large charge symmetry violation. In a recent Letter [14] we argued that the data supported this conclusion. However, several important corrections have to be applied to the data before any conclusions can be reached. These corrections are especially important for the neutrino cross sections.

In Sec. II we discuss the uncertainties involved in the analysis of the data. Most corrections have already been accounted for in the present experimental analysis. We particularly focus on two aspects of the neutrino reactions: heavy target corrections and effects due to strange and antistrange quark distributions. In Sec. III we demonstrate that neither of these effects are sufficient to account for the apparent discrepancy at small x. The charge symmetry violating distributions can be obtained from a combination of neutrino charged current structure functions, muon structure functions

and strange quark distributions extracted from dimuon production in neutrino reactions. We construct such a combination and extract the CSV terms. Assuming the validity of the experimental data, we find CSV effects on the order of 25% of the sea quark distributions at low x. In Sec. IV we discuss the consequences of such large CSV effects on other observables. We examine the role played by CSV in the extraction of the FSV ratio $\overline{d}/\overline{u}$, in the Gottfried sum rule and in the experimental determination of the Weinberg angle $\sin^2\theta_W$. In Sec. V we suggest an experiment which could measure the substantial CSV suggested by our analysis.

II. COMPARING STRUCTURE FUNCTIONS FROM NEUTRINO AND CHARGED LEPTON REACTIONS

Our analysis of parton charge symmetry violation is based on the ''charge ratio,'' which we review here. This depends on the ratio of F_2 structure functions extracted from charged lepton reactions with those from neutrino charge-changing reactions. Because neutrino cross sections are so small, at present the structure functions can only be measured for heavy targets such as iron. Furthermore, in order to obtain useful statistics, the data must be integrated over all energies for a given x and Q^2 bin. As a result, only certain linear combinations of neutrino and antineutrino structure functions can be obtained. The process by which we attempt to extract parton CSV contributions is complicated, and requires input from several experiments. In this section we review this process in detail.

A. The ''charge ratio'' and charge symmetry violation

Structure functions measured in neutrino and muon deep inelastic scattering are interpreted in terms of parton distribution functions. Since the operation of charge symmetry maps up quarks to down quarks, and protons to neutrons, at the level of parton distributions, charge symmetry implies the equivalence between up (down) quark distributions in the proton and down (up) quark distributions in the neutron. In order to take CSV in the parton distributions into account, we define the charge symmetry violating distributions as

$$\delta u(x) = u^p(x) - d^n(x)$$

$$\delta d(x) = d^p(x) - u^n(x), \tag{1}$$

where the superscripts p and n refer to quark distributions in the proton and neutron, respectively. The relations for CSV in antiquark distributions are analogous. If charge symmetry were exact then the quantities $\delta u(x)$ and $\delta d(x)$ would vanish.

In the quark-parton model the structure functions measured in neutrino, antineutrino and charged lepton DIS on an isoscalar target, N_0, are given in terms of the parton distribution functions and the charge symmetry violating distributions defined above by [3]

$$\begin{aligned}
F_2^{\nu N_0}(x,Q^2) &= x[u(x)+\overline{u}(x)+d(x)+\overline{d}(x)+2s(x)+2\overline{c}(x) \\
&\quad -\delta u(x)-\delta\overline{d}(x)] \\
F_2^{\overline{\nu} N_0}(x,Q^2) &= x[u(x)+\overline{u}(x)+d(x)+\overline{d}(x)+2\overline{s}(x)+2c(x) \\
&\quad -\delta d(x)-\delta\overline{u}(x)] \\
xF_3^{\nu N_0}(x,Q^2) &= x[u(x)+d(x)-\overline{u}(x)-\overline{d}(x)+2s(x)-2\overline{c}(x) \\
&\quad -\delta u(x)+\delta\overline{d}(x)] \\
xF_3^{\overline{\nu} N_0}(x,Q^2) &= x[u(x)+d(x)-\overline{u}(x)-\overline{d}(x)-2\overline{s}(x)+2c(x) \\
&\quad -\delta d(x)+\delta\overline{u}(x)] \\
F_2^{lN_0}(x,Q^2) &= \frac{5}{18}x\Big[u(x)+\overline{u}(x)+d(x)+\overline{d}(x) \\
&\quad +\frac{2}{5}(s(x)+\overline{s}(x))+\frac{8}{5}(c(x)+\overline{c}(x)) \\
&\quad -\frac{4}{5}(\delta d(x)+\delta\overline{d}(x))-\frac{1}{5}(\delta u(x)+\delta\overline{u}(x))\Big].
\end{aligned} \tag{2}$$

Here, and in the following, quark distributions without superscripts denote quark distributions in the proton. From now on, we will disregard charm quark contributions to the structure functions. Since phenomenological parton distribution functions assume the validity of charge symmetry, possible CSV effects are folded into the commonly used phenomenological parton distribution functions in a highly non-trivial way. Nevertheless, using the above relations, it is possible to test the validity of charge symmetry by building appropriate linear combinations or ratios of the measured structure functions. One such possibility is to calculate the ''charge ratio,'' which relates the neutrino structure function to the structure function measured in charged lepton deep-inelastic scattering:

$$\begin{aligned}
R_c(x,Q^2) &\equiv \frac{F_2^{\mu N_0}(x,Q^2)}{\frac{5}{18}F_2^{\nu N_0}(x,Q^2)-x(s(x)+\overline{s}(x))/6} \\
&\approx 1-\frac{s(x)-\overline{s}(x)}{\overline{Q}(x)} \\
&\quad +\frac{4\,\delta u(x)-\delta\overline{u}(x)-4\,\delta d(x)+\delta\overline{d}(x)}{5\overline{Q}(x)}.
\end{aligned} \tag{3}$$

Here, we defined $\overline{Q}(x)\equiv\Sigma_{q=u,d,s}(q(x)+\overline{q}(x))-3(s(x)+\overline{s}(x))/5$, and we have expanded Eq. (3) to lowest order in small quantities. From Eq. (3) we see that any deviation of the charge ratio from unity, at any value of x, would be due either to CSV effects or to different strange and antistrange

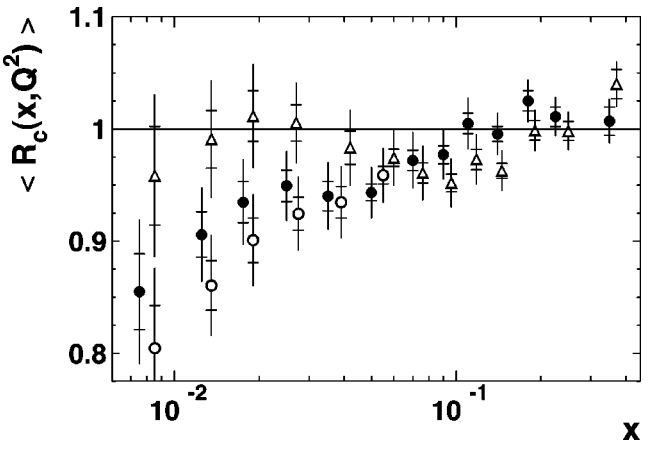

FIG. 1. The ''charge ratio'' R_c of Eq. (3) vs x calculated using CCFR [13] data for neutrino and NMC [12] data for muon structure functions. Open triangles: no heavy target corrections; open circles: ν data corrected for heavy target effects using corrections from charged lepton scattering; solid circles: ν shadowing corrections calculated in the ''two phase'' model. Both statistical and systematic errors are shown.

quark distributions. Analogous relations could be obtained using structure functions from antineutrinos, or from a linear combination of neutrino and antineutrino structure functions. For example, we can derive

$$\mathcal{R}_c(x,Q^2) \equiv \frac{F_2^{\mu N_0}(x,Q^2)}{\frac{5}{18}\mathcal{F}_2^{\nu N_0}(x,Q^2) - x(s(x)+\overline{s}(x))/6} \approx 1 + \frac{3(\delta u(x) + \delta\overline{u}(x) - \delta d(x) - \delta\overline{d}(x))}{10\overline{Q}(x)}. \quad (4)$$

In Eq. (4) $\mathcal{F}_2^{\nu N_0}(x,Q^2) = (F_2^{\nu N_0}(x,Q^2) + F_2^{\overline{\nu} N_0}(x,Q^2))/2$ is the average of the structure functions from neutrino and antineutrino reactions; deviations from one in the ratio $\mathcal{R}_c(x)$ depend only on parton CSV contributions, and have no contribution from strange or antistrange quark distributions.

The recent measurement of the structure function F_2^ν by the CCFR Collaboration [13] makes it possible to carry out a precise comparison between $F_2^\nu(x,Q^2)$ and $F_2^\mu(x,Q^2)$ for the first time. The CCFR Collaboration compared the neutrino structure function $F_2^\nu(x,Q^2)$ extracted from their data on an iron target [13] with $F_2^\mu(x,Q^2)$ measured for the deuteron by the NMC Collaboration [12]. In the region of intermediate values of Bjorken x ($0.1 \leqslant x \leqslant 0.4$), they found very good agreement between the two structure functions. In this x region, this allows us to set upper limits of a few percent on parton CSV contributions. On the other hand, in the small x-region ($x < 0.1$), the CCFR group found that the two structure functions differ by as much as 10–15 %. This can be seen in Fig. 1 where the ''charge ratio'' has been obtained by integrating over the region of overlap in Q^2 of the two experiments. The open and solid circles in Fig. 1 represent two different ways of calculating nuclear shadowing corrections, as we will discuss later.

B. Extracting structure functions from neutrino cross sections

In order to perform tests of parton distributions through, say, the charge ratio of Eq. (3), we need the structure functions from neutrino charge-changing reactions on a free proton and neutron. These are written in terms of parton distributions in Eq. (2). Because of the extremely small cross sections for neutrino-induced reactions, we are able to obtain statistically meaningful cross sections only from heavier targets such as iron. We then have to make the following corrections in order to extract the neutrino structure functions on ''free'' nucleons, averaged over proton and neutron, $F_j^{\nu,\overline{\nu}N_0}(x,Q^2)$, $(j=2,3)$: (i) the nuclear structure functions $F_j^{\nu,\overline{\nu}Fe}(x,Q^2)$ must be extracted from the cross sections; (ii) the nuclear structure functions need to be corrected for the excess of neutrons in iron (isoscalar effects); (iii) kinematic corrections must be applied to account for heavy quark thresholds, particularly charm quark threshold effects [Eq. (3) is valid only well above all heavy quark thresholds]; (iv) heavy target corrections must be applied, to convert structure functions for nuclei to those for free protons and neutrons; (v) the neutrino and muon cross sections must be properly normalized. In order to test charge symmetry, all these corrections have to be taken into account. The data have already been corrected for normalization, isoscalar and charm threshold effects by the CCFR Collaboration in their analyses [13]. There is a thorough discussion of these points in the thesis by Seligman [15]. Here we will review how the nuclear structure functions are extracted from the cross sections, the heavy target corrections for neutrino reactions, and the role of both strange quarks and CSV effects in neutrino structure functions.

The cross sections for neutrino and antineutrino scattering on a nuclear target containing A nucleons can be written as

$$\frac{d\sigma^{\nu,\overline{\nu}A}}{dx\,dQ^2} = \frac{G_F^2}{2\pi x}\left[\frac{1}{2}(F_2^{\nu,\overline{\nu}A}(x,Q^2) \pm xF_3^{\nu,\overline{\nu}A}(x,Q^2)) + \frac{\xi^2}{2}(F_2^{\nu,\overline{\nu}A}(x,Q^2) \mp xF_3^{\nu,\overline{\nu}A}(x,Q^2))\right]. \quad (5)$$

In Eq. (5) the upper (lower) sign is associated with the neutrino (antineutrino) cross section. We have assumed the validity of the Callan-Gross relation and neglected terms of order $Mxy/2E$, and we introduced the variable $\xi = (1-y)$. It would be straightforward to remove these assumptions. With a large enough count rate, the x and y dependence of the cross sections could be separately measured. By plotting the measured differential cross sections for fixed x and Q^2 as a function of ξ^2, the structure functions F_2 and F_3 can be determined from the slopes and intercepts of the resulting straight lines. The crucial question is, of course, whether the statistics of the experiment are sufficient for the structure functions to be extracted in this way.

To illustrate this problem we calculated the statistical errors in each energy bin. For this calculation, we used the experimental determined fluxes, the total and differential neutrino and antineutrino cross sections to obtain the expected number of events in a given x, Q^2 and energy bin. We

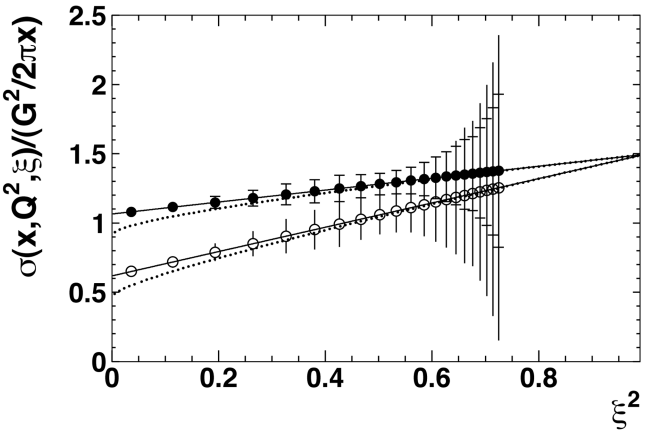

FIG. 2. The differential cross sections for neutrino (solid circles) and antineutrino (open circles) deep inelastic scattering as a function of the variable $\xi^2 \equiv (1-y)^2$ for $x=0.03$ and $Q^2=4$ GeV^2. The solid and dotted lines are the results with and without the Callan-Gross relation, respectively. The statistical errors are estimated using the experimental fluxes of neutrinos and antineutrinos.

estimated the statistical errors using $\Delta\sigma=\sigma/\sqrt{N}$. In Fig. 2 $\sigma^{\nu,\bar{\nu}}(x,Q^2,\xi^2)/(G_F^2/2\pi x)$ is plotted as a function of ξ^2. The solid lines are the results using the CTEQ parton distribution functions and assuming the validity of the Callan-Gross relation. The dotted lines are the results obtained without using the Callan-Gross relation. Here, we used the parametrization of Whitlow [16] for the ratio of the longitudinal and transverse photo-absorption cross sections. The current statistics do not allow one to extract the individual structure functions. The error bars represent the expected statistical errors. An order of magnitude more events would be necessary to decrease the statistical errors sufficiently that one could consider extracting the structure functions directly, and systematic errors would further complicate this analysis.

Since the number of events is so small that individual structure functions cannot be extracted from the data, the cross sections in a given x and Q^2 bin are integrated over all energies. After this integration is performed, Eq. (5) can be written as two linear equations, one for neutrino and the other for antineutrino events:

$$N^{\nu}(x,Q^2)=A_2^{\nu}F_2^{\nu Fe}(x,Q^2)+A_3^{\nu}xF_3^{\nu Fe}(x,Q^2)$$

$$N^{\bar{\nu}}(x,Q^2)=A_2^{\bar{\nu}}F_2^{\bar{\nu}Fe}(x,Q^2)-A_3^{\bar{\nu}}xF_3^{\bar{\nu}Fe}(x,Q^2). \tag{6}$$

In Eq. (6) N^{ν} ($N^{\bar{\nu}}$) is the number of neutrino (antineutrino) events in a given x and Q^2-bin integrated over the incident neutrino and antineutrino energies. A_i^{ν} and $A_i^{\bar{\nu}}$ ($i=2,3$) represent the coefficients, $A_i(y)$, of the structure functions multiplied by the neutrino and antineutrino fluxes, $\Phi^{\nu}(E)$ and $\Phi^{\bar{\nu}}(E)$, respectively, and integrated over all energies

$$A_i^{\nu}=\int dE\, A_i(y)\Phi^{\nu}(E)$$

$$A_i^{\bar{\nu}}=\int dE\, A_i(y)\Phi^{\bar{\nu}}(E). \tag{7}$$

Here, the A_i's are given by $A_2(y)=G_F^2/(2\pi x)(1-y+y^2/2)$ and $A_3(y)=G_F^2/(2\pi x)(y-y^2/2)$.

The individual structure functions for neutrino and antineutrino reactions are extracted by taking linear combinations of the relations in Eq. (6) and making corrections using phenomenological parton distribution functions. For example, from Eq. (2) we see that for an isoscalar target, $F_2^{\nu N_0}(x,Q^2)=F_2^{\bar{\nu}N_0}(x,Q^2)$ if charge symmetry is valid and $s(x)=\bar{s}(x)$. Thus we can form linear combinations of the terms in Eq. (6) such that these terms cancel and we are left only with the F_3 structure functions. Similarly, assuming charge symmetry we have

$$F_3^{\nu N_0}(x,Q^2)-F_3^{\bar{\nu}N_0}(x,Q^2)=2[s(x)-\bar{s}(x)].$$

We can then take a linear combination of the terms in Eq. (6) which gives this function. If the strange quark distribution is taken from a phenomenological model, we can extract a linear combination of the F_2 structure functions for neutrinos and antineutrinos on a nuclear target.

We will discuss how the structure functions are extracted, and particularly the role of CSV and strange quark distributions in this process. However, at this stage we review how heavy target corrections are calculated, in order to extract the structure functions for free nucleons from those measured on a heavy nuclear target.

C. Heavy target corrections in neutrino reactions

As is well known, the structure functions measured on heavy targets are not equal to those observed for light targets such as the deuteron. At small x values, nuclear shadowing effects play a major role; at large x, nuclear Fermi motion effects dominate, and at intermediate x ''EMC'' effects play a significant role [17]. Such effects have been systematically measured in charged lepton reactions.

In analyzing neutrino scattering data, it is generally assumed that heavy target corrections will be the same as those observed in charged lepton reactions. *A priori*, there is no reason to assume that neutrino and charged lepton heavy target corrections should be identical. Heavy target corrections for neutrinos are generally applied by multiplying the experimental structure functions at a given x value by the quantity $R \equiv F_2^{lA}(x,Q^2)/F_2^{lD}(x,Q^2)$, the ratio between the F_2 structure function measured on heavy targets and that of the deuteron for charged lepton deep inelastic scattering, at the same x value. However, as is well known, shadowing corrections are very much Q^2 dependent for smaller Q^2 values (where a considerable part of the available data was taken), and the Q^2 and x-dependence of the data are strongly correlated because of the fixed target nature of these experiments.

We re-examined heavy target corrections to deep-inelastic neutrino scattering, focusing on the differences between neutrino and charged lepton scattering and on effects due to the Q^2-dependence of shadowing for moderately large Q^2. This work will be published elsewhere [18]; here we briefly review the results of that work. We used a two phase model which has been successfully applied to the description of shadowing in charged lepton DIS [19,20]. In this approach, vector meson dominance is used to describe the low Q^2 virtual photon or W interactions, and Pomeron exchange is used for the approximate scaling region. In generalizing this approach to weak currents, the essential differences in shadowing between neutrino and charged lepton deep inelastic scattering are: (i) the axial-vector current is only partially conserved, in contrast to the vector current; and (ii) the weak current couples not only to vector but also to axial vector mesons [21–24].

Partial conservation of the axial vector current (PCAC) requires that the divergence of the axial current does not vanish but is proportional to the pion field for $Q^2=0$. This is Adler's theorem [25], which relates the neutrino cross section to the pion cross section on the same target for $Q^2=0$. Thus, for low $Q^2(\approx m_\pi^2)$ shadowing in neutrino scattering is determined by the absorption of pions on the target. For larger Q^2-values the contributions of vector and axial vector mesons become important. The coupling of the weak current to the vector and axial vector mesons and that of the electromagnetic current to vector mesons are related to each other by the ''Weinberg sum rule'' $f_{\rho^+}^2=f_{a_1}^2=2f_{\rho^0}^2$. Since the coupling of the vector (axial vector) mesons to the weak current is twice as large as the coupling to the electro-magnetic current, but the structure function is larger by a factor of $\sim 18/5$ in the neutrino case, we expect that shadowing due to vector meson dominance (VMD) in neutrino reactions is roughly half of that in charged lepton scattering.

For larger Q^2 values, shadowing due to Pomeron exchange between the projectile and two or more constituent nucleons dominates. Since the Pomeron-exchange models the interaction between partons in different nucleons and the scattering of the W takes place on only one parton, this process is of leading twist order in contrast to the VMD and pion contributions. The coupling is given by the coupling of the photon or W to the quarks in the exchanged Pomeron. It changes in the same way as the structure function does in switching from neutrino to charged lepton scattering. Thus, for large Q^2 values (>10 GeV^2), shadowing in both cases should have approximately the same magnitude. In the intermediate Q^2-region ($1<Q^2<10$ GeV^2), where VMD is relatively important, we expect to see differences between shadowing in neutrino and charged lepton scattering. We recall that this is precisely the region where the discrepancy between CCFR and NMC is significant. There are also nuclear effects in the deuteron. However, because of the low density of the deuteron, these are (relatively speaking) very small and have a negligible effect on the charge ratio.

We calculated the shadowing corrections to the CCFR neutrino data using the two-phase model of Refs. [19,20]. With this corrected CCFR data, we calculated the charge ratio R_c of Eq. (3) between CCFR and NMC data. The result is shown in Fig. 1. The open triangles show the charge ratio when no shadowing corrections are used. The open circles show the charge ratio when heavy target shadowing corrections from charged lepton reactions are applied to the neutrino data, and the solid circles show the result when the neutrino shadowing corrections from our two-phase model are applied. At small x, using the ''correct'' neutrino shadowing corrections reduces the deviation of the charge ratio from unity. Nevertheless, the charge ratio is still not compatible with one at small x. The uncertainty in the calculated shadowing corrections can be estimated. The model describes shadowing in charged lepton DIS for a wide range of x and Q^2 values and for different nuclei very well. Changing parameters of the model, i.e. the vector meson-photon coupling constants, by 10% over/underestimates shadowing by about 10%. Since shadowing corrections are at most 15% of the structure function the uncertainty in the corrected charge ratio is about 1.5 percent.

In summary, properly accounting for shadowing corrections in the neutrino structure function decreases, but does not resolve, the low-x discrepancy between the CCFR and the NMC data.

D. Strange quark and CSV contributions to structure functions

In Eq. (6) we showed that, after integrating neutrino charged-current cross sections over all energies, we obtain two equations in four unknowns, the structure functions F_2 and F_3 for neutrino and antineutrino reactions. If the neutrino and antineutrino structure functions were equal, $F_2^{\nu Fe}(x,Q^2)=F_2^{\bar{\nu}Fe}(x,Q^2)$, with an analogous relation for $xF_3^{\nu Fe}(x,Q^2)$, then Eq. (6) would provide two linear equations in two unknowns. As we discussed previously, several corrections need to be applied before we can extract the structure functions on a ''free'' isoscalar target N_0, and compare the structure functions to the parton distributions given in Eq. (2). First, since iron is not an isoscalar target we need to make corrections for the excess neutrons. Next, we need to estimate the contributions from strange quark distributions and charge symmetry violating parton distributions. Finally, we need to make heavy target corrections as reviewed in the preceding section.

We begin by splitting the neutrino and antineutrino structure functions on iron into isoscalar and non-isoscalar parts. For a target with Z protons and $N=A-Z$ neutrons we define the quantity $\beta\equiv(N-Z)/A$:

$$F_i^{\nu,\bar{\nu}Fe}=\frac{1}{2}[F_i^{\nu,\bar{\nu}p}+F_i^{\nu,\bar{\nu}n}]-\frac{\beta}{2}[F_i^{\nu,\bar{\nu}p}-F_i^{\nu,\bar{\nu}n}]. \qquad (8)$$

The first term on the right of Eq. (8) corresponds to the neutrino and antineutrino structure functions on an isoscalar target, N_0. The second terms include corrections arising from the non-isoscalarity of the target. In the absence of CSV, these corrections are basically given by the difference between up and down valence quark distributions and have

been taken into account in the extraction of the structure functions. However, the non-isoscalarity of the target leads also to CSV corrections.

We define the sum and difference of the neutrino and antineutrino structure functions on a target A as

$$\mathcal{F}_i^A \equiv \frac{1}{2}[F_i^{\nu A} + F_i^{\bar{\nu} A}],$$

$$\Delta\mathcal{F}_i^A \equiv \frac{1}{2}[F_i^{\nu A} - F_i^{\bar{\nu} A}]; \tag{9}$$

the structure functions $F_i^{\nu,\bar{\nu}Fe}$ can then be written as

$$F_i^{\nu,\bar{\nu}Fe} = \mathcal{F}_i^{N_0} \pm \Delta\mathcal{F}_i^{N_0} - \frac{\beta}{2}\{[\mathcal{F}_i^p - \mathcal{F}_i^n] \pm [\Delta\mathcal{F}_i^p - \Delta\mathcal{F}_i^n]\}. \tag{10}$$

Here, ''+'' and ''−'' refer to the neutrino and antineutrino structure functions, respectively. The last three terms of the right hand side of Eq. (10) contain corrections coming from excess neutrons, strange quarks, CSV and $s(x) \neq \bar{s}(x)$. Correcting the data for excess neutrons and for strange quark contributions corresponds to subtracting the number of events due to the corresponding corrections from the left hand side of Eqs. (6):

$$N^\nu - \sum_{i=2}^{3} A_i^\nu (\delta\mathcal{F}_i^\nu)_{n,s} = A_2^\nu [\mathcal{F}_2^{N_0} + (\delta\mathcal{F}_2^\nu)_{CSV}^{s\bar{s}}] + A_3^\nu x [\mathcal{F}_3^{N_0} + \delta(\mathcal{F}_3^\nu)_{CSV}^{s\bar{s}}]$$

$$N^{\bar{\nu}} - \sum_{i=2}^{3} (-1)^i A_i^{\bar{\nu}} (\delta\mathcal{F}_i^{\bar{\nu}})_{n,s} = A_2^{\bar{\nu}} [\mathcal{F}_2^{N_0} + (\delta\mathcal{F}_2^{\bar{\nu}})_{CSV}^{s\bar{s}}] - A_3^{\bar{\nu}} x [\mathcal{F}_3^{N_0} + (\delta\mathcal{F}_3^{\bar{\nu}})_{CSV}^{s\bar{s}}]. \tag{11}$$

In Eq. (11), we have calculated corrections to the structure functions from excess neutrons and strange quarks, and have used these to produce the effective number of events on the left hand side of Eq. (11). $(\delta\mathcal{F}_i)_{n,s}$ and $(\delta\mathcal{F}_i)_{CSV}^{s\bar{s}}$ refer to corrections arising from excess neutrons, strange quark distributions, because of charge symmetry violation and $s(x) \neq \bar{s}(x)$, respectively. The CCFR Collaboration assumed the validity of charge symmetry, and they also took $s(x) = \bar{s}(x)$ based on the results of a next to leading order [NLO] analysis of dimuon production in neutrino-induced reactions [26]. We have left the correction terms coming from CSV and $s(x) \neq \bar{s}(x)$ on the right hand side of Eq. (6) as these have been absorbed into the extracted structure functions. Under the assumption of charge symmetry and $s(x) = \bar{s}(x)$, Eq. (11) simplifies to

$$N^\nu - \sum_{i=2}^{3} A_i^\nu (\delta\mathcal{F}_i^\nu)_{n,s} = A_2^\nu \mathcal{F}_2^{CCFR,A} + A_3^\nu x \mathcal{F}_3^{CCFR,A}$$

$$N^{\bar{\nu}} - \sum_{i=2}^{3} (-1)^i A_i^{\bar{\nu}} (\delta\mathcal{F}_i^{\bar{\nu}})_{n,s} = A_2^{\bar{\nu}} \mathcal{F}_2^{CCFR,A} - A_3^{\bar{\nu}} x \mathcal{F}_3^{CCFR,A}. \tag{12}$$

These equations provide a system of two linear equations for the two nuclear structure functions $\mathcal{F}_2^{CCFR,A}$ and $\mathcal{F}_3^{CCFR,A}$. From these structure functions we can calculate the structure functions for a ''free'' nucleon target using the heavy target correction factors described in the previous section. The resulting structure functions $\mathcal{F}_i^{CCFR}$ still contain charge symmetry violating contributions and terms proportional to $s(x) - \bar{s}(x)$, as can be seen from Eq. (2). To relate the measured structure functions, F_i^{CCFR} to the various parton distributions, we take the sum and difference of the measured number densities in Eqs. (11) and (12) and compare the coefficients of $A_i(y)$ (powers of y). In this way, we see that the measured structure functions, F_i^{CCFR}, can effectively be identified with a flux weighted average of the neutrino and antineutrino structure functions, $F_i^{\nu N_0}$ and $F_i^{\bar{\nu} N_0}$, and correction terms arising from CSV effects:

$$F_i^{CCFR} = \mathcal{F}_i^{N_0} + (2\alpha - 1)\Delta\mathcal{F}_i^{N_0} - \frac{\beta}{2}[\mathcal{F}_i^p - \mathcal{F}_i^n]_{CSV} - \frac{(2\alpha-1)\beta}{2}[\Delta\mathcal{F}_i^p - \Delta\mathcal{F}_i^n]_{CSV}. \tag{13}$$

Here, we defined the relative neutrino flux, α, as $\alpha \equiv \Phi^\nu/(\Phi^\nu + \Phi^{\bar{\nu}})$. The experimental value of α depends on the incident neutrino and antineutrino energies and is also different for the E744 and E770 experiments. Because of the kinematical constraint $y < 1$, relative fluxes at energies $\geqslant 150$ GeV are relevant for small x. Here, $\alpha \approx 0.83$ [13] so that $F_2^{CCFR}(x, Q^2)$ can be approximately regarded as a neutrino structure function.

The different contributions to F_2^{CCFR} can be expressed in terms of the quark distribution functions:

$$\frac{1}{2}[\mathcal{F}_2^p - \mathcal{F}_2^n]_{CSV} = -[\mathcal{F}_2^{N_0}]_{CSV} = \frac{x}{2}[\delta u(x) + \delta\bar{u}(x) + \delta d(x) + \delta\bar{d}(x)]$$

$$\frac{1}{2}[\Delta\mathcal{F}_2^p - \Delta\mathcal{F}_2^n]_{CSV} = -\frac{x}{2}[\delta d(x) - \delta\bar{d}(x) - \delta u(x) + \delta\bar{u}(x)]$$

$$\Delta\mathcal{F}_2^{N_0} = -\frac{1}{2}[\Delta\mathcal{F}_2^p - \Delta\mathcal{F}_2^n]_{CSV} + x[s(x) - \bar{s}(x)]. \tag{14}$$

The second expression in Eq. (14) is obtained by subtracting the F_2 structure function for neutrinos on protons from that for antineutrinos on protons; from this is subtracted the corresponding term for neutrons. It depends only on charge symmetry violation in the *valence* quark distributions. The last expression in Eq. (14) is obtained by taking the difference between neutrino and antineutrino F_2 structure functions on an isoscalar system. It also depends on valence quark CSV, and has an additional contribution from the difference between strange and antistrange parton distributions. The first term in Eq. (14) is obtained by averaging the F_2 structure functions over neutrino and antineutrino reactions, and taking the difference of the F_2 structure functions measured on proton and neutron targets. This quantity is free from strange quark effects, and is also sensitive to CSV in the sea-quark distributions.

III. EVIDENCE FOR LARGE CHARGE SYMMETRY VIOLATION IN PARTON SEA QUARK DISTRIBUTIONS

The most likely explanation for the discrepancy in the small-x region of the charge ratio involves either differences between the strange and antistrange quark distributions [27–30], or charge symmetry violation. First, we will examine the role played by the strange and antistrange quark distributions. Assuming that charge symmetry is exact, the strange and antistrange quark distributions are given by a linear combination of the structure functions measured in neutrino and in muon DIS, as can be seen from Eqs. (2), (13) and (14):

$$\frac{5}{6}F_2^{CCFR}(x,Q^2)-3F_2^{NMC}(x,Q^2) = \frac{1}{2}x[s(x)+\overline{s}(x)]+\frac{5}{6}(2\alpha-1)x[s(x)-\overline{s}(x)]. \quad (15)$$

Here, it understood that the neutrino structure function, F_2^{CCFR} is already corrected for heavy target effects. Under the assumption that $s(x)=\overline{s}(x)$, this relation could be used to extract the strange quark distribution. However, as is well known, the strange quark distribution obtained in this way is inconsistent with the distribution extracted from independent experiments.

A. Direct measurement of sea quark distributions

The strange quark distribution can be determined directly from opposite sign dimuon production in deep inelastic neutrino and antineutrino scattering. To leading order in a charge-changing reaction, the incoming neutrino (antineutrino) emits a muon and a virtual W boson, which scatters on an s or d ($\overline{s}$ or $\overline{d}$) quark, producing a charm (anticharm) quark which fragments into a charmed hadron. The semi-leptonic decay of the charmed hadron produces an opposite sign muon. The CCFR Collaboration performed a LO [31] and NLO analysis [26] of their dimuon data using the neutrino (antineutrino) events to extract the strange (antistrange) quark distributions. Their result differs substantially from the strange quark distribution extracted from Eq. (15), as mentioned above.

In the dimuon data one extracts the strange and antistrange quark distributions from the neutrino and antineutrino data separately. The analysis performed by the CCFR Collaboration suggests that, while there is a difference between the strange and antistrange distributions in LO analysis [31] they are equal within experimental errors in NLO [26]. However, since the number of antineutrino events is much smaller than that of the neutrino events, the errors of this analysis are inevitably large.

Since the dimuon experiments are carried out on an iron target, shadowing corrections could modify the extracted strange quark distribution, and might account for some of the discrepancies between the two different determinations of the strange quark distributions. The CCFR Collaboration normalized the dimuon cross section to the ''single muon'' cross section and argued that the heavy target correction should cancel in the ratio. However, the charm producing part of the structure function $F_2^{cp}(x,Q^2)$ could be shadowed differently from the non-charm producing part $F_2^{ncp}(x,Q^2)$, unless charm threshold effects cancel in the shadowing ratio. This could be the case, because vector mesons with higher masses are involved in the charm producing part, and because charm production threshold effects have to be taken into account in the Pomeron component as well.

We calculated the shadowing ratio, $R \equiv F_2^{\nu A}(x,Q^2)/F_2^{\nu D}(x,Q^2)$, between the structure functions on a heavy target and on a deuteron target for both the charm and non-charm producing part of the structure function. We took charm production threshold effects into account in the Pomeron component through the slow rescaling mechanism by replacing x_{P} by the rescaled variable $\xi_{\mathrm{P}}=x_{\mathrm{P}}(1+m_c^2/Q^2)$. Here, $x_{\mathrm{P}}\equiv x/y_{\mathrm{P}}$ is the fraction of the Pomeron's momentum carried by the struck quark, y_{P} is the fraction of the momentum of the nucleon carried by Pomeron and m_c is the mass of the charm quark. In the VMD component of $F_2^{cp}(x,Q^2)$ we included the vector mesons $D^{*+}(2010)$, $D_s^{*+}(2110)$ and the axial vector partner $D_{As}^{*+}(2535)$ of D_s^{*+} [32], which describe the lightest coherent states of the $c\overline{d}$ and $c\overline{s}$ fluctuations of the W^+ boson. They have the same coupling to W^+ as ρ^+ and a_1^+ but have much heavier masses. (The $c\overline{d}$ fluctuations are suppressed by $\sin^2\Theta_c$.) The total shadowing in the two phase model is the sum of the contributions from the Pomeron and vector meson components. While the vector meson component is of higher twist and decreases with increasing Q^2 the Pomeron component dominates at high Q^2. In the transition region, adding the two components can lead to double counting. This problem could in principle be avoided by keeping only the leading twist piece of the Pomeron structure function. Here, we adapt the alternative solution of Kwiecinski and Badelek [19] and exclude from the Pomeron exchange component those final states X which have masses comparable to the relevant vector meson masses. Since the mass of the charmed vector mesons ($\sim$2.5 GeV), we applied a cut at $M_X^2 \geqslant 6.3$ GeV^2 in the diffractively produced invariant mass of

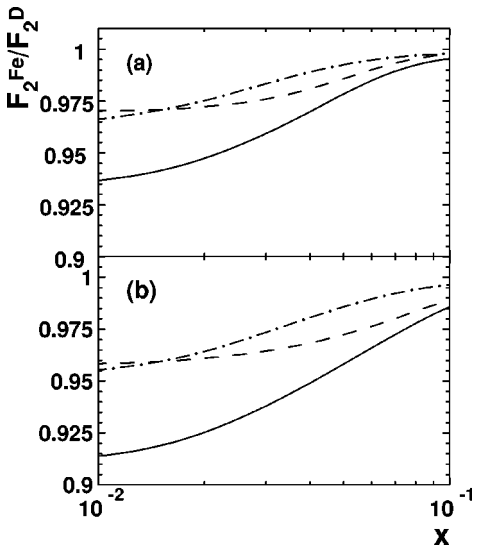

FIG. 3. Shadowing corrections in the (a) charm and (b) non-charm producing parts of the neutrino structure function, as a function of x, for a fixed $Q^2=5$ GeV^2. The dashed (dash-dotted) lines stand for VMD (Pomeron) contributions. The solid lines represent the total shadowing.

the Pomeron component. Because of the *light* quark component of the D-mesons, we expect that the D-meson-nucleon total cross sections are comparable to the corresponding cross sections of lighter mesons with the same light quark content. We use $\sigma_{D*N}\approx\sigma_{\rho N}$ and $\sigma_{D_s^*N}\approx\sigma_{\phi N}$. The calculated ratios, $R=F_2^A(x,Q^2)/F_2^D(x,Q^2)$, are shown in Fig. 3 for $Q^2=5$ GeV^2. Here, $F_2^A=F_2^D+\delta F_2^V+\delta F_2^{\mathbb{P}}$ and δF_2^V and $\delta F_2^{\mathbb{P}}$, the shadowing corrections to the structure functions due to vector mesons and Pomeron exchange, respectively, are calculated in the two phase model. Since the pion component is negligible for $Q^2=5$ GeV^2, we did not include it.

There is no substantial difference in shadowing between the charm producing (cp) and non-charm producing (ncp) parts. (The difference is about 2% in the small x region.) Note that the shadowing correction in $F_2^{cp}(x,Q^2)$ decreases faster with increasing x, because the larger masses of the charmed vector mesons, m_V, enter in the coherence condition $\tau=(1/Mx)(1+(m_V^2/Q^2))^{-1}$ (τ is the lifetime of the quark antiquark fluctuation, and M is the nucleon mass), compared with the smaller masses of the ρ and a_1. Our results justify the assumption that shadowing corrections approximately cancel in the ratio of dimuon and single muon cross sections.

B. Estimate of parton CSV contribution

It would appear that a likely explanation for the deviation of the charge ratio of Eq. (3) from one is due to differences between the strange and antistrange quark densities. To test this hypothesis, we combined the data in dimuon production, averaged over both neutrino and antineutrino events, with the difference between the structure functions in neutrino and charged lepton scattering [Eq. (15)]. Note, that in Eq. (15) F_2^{CCFR} is already corrected for heavy target effects. Thus, we test the effects of $s(x)\neq\bar{s}(x)$ *in addition* to shadowing. In combining the neutrino and antineutrino events, one measures a flux-weighted average of the strange and antistrange quark distributions. If we define $\alpha'=N_\nu/(N_\nu+N_{\bar\nu})$, where $N_\nu=5030, N_{\bar\nu}=1060$ ($\alpha'\approx0.83$) are the number of neutrino and antineutrino events of the dimuon production experiment [26], we have for the measured distribution $xs(x)^{\mu\mu}$

$$xs^{\mu\mu}(x)=\frac{1}{2}x[s(x)+\bar{s}(x)]+\frac{1}{2}(2\alpha'-1)x[s(x)-\bar{s}(x)]. \tag{16}$$

Now, this equation together with Eq. (15) forms a pair of linear equations which can be solved for $\frac{1}{2}x[s(x)+\bar{s}(x)]$ and $\frac{1}{2}x[s(x)-\bar{s}(x)]$. In this way we can also test the compatibility of the two experiments. In addition we have the sum rule that the nucleon contains no net strangeness,

$$\int_0^1[s(x)-\bar{s}(x)]dx=0. \tag{17}$$

In the following expressions, we have not enforced the sum rule requirement on the antistrange quark distributions.

Compatibility of the two experiments requires that physically acceptable solutions for $\frac{1}{2}x[s(x)+\bar{s}(x)]$ and $\frac{1}{2}x[s(x)-\bar{s}(x)]$, satisfying both Eq. (15) and Eq. (16), can be found. Using the experimental values $\alpha=\alpha'\approx0.83$, we can write $x[s(x)-\bar{s}(x)]=\Delta(x)/\delta$, where $\Delta(x)=\frac{5}{6}F_2^{CCFR}(x)-3F_2^{NMC}(x)-s^{\mu\mu}(x)$, and $\delta=(2\alpha-1)/3\approx0.22$. Consequently even rather small values for $\Delta(x)$ can lead to large differences between s and $\bar{s}$. Note that the value of the relative neutrino flux, α, depends on the incident neutrino energy. While $\alpha\approx0.83$ for small x, α is somewhat smaller for higher x-values. However, smaller α would lead to an even smaller δ and would require even larger differences between s and $\bar{s}$.

In Fig. 4 we show the results obtained for $xs(x)$ (open circles) and $x\bar{s}(x)$ (solid circles) by solving the resulting linear equations, Eqs. (15) and (16) using the values $\alpha=\alpha'=0.83$. The results are completely unphysical, since the antistrange quark distribution is negative, which is not possible since the distribution is related to a probability. In Fig. 5 we show the corresponding results for the linear combinations $\frac{1}{2}x[s(x)+\bar{s}(x)]$ (solid circles) and $\frac{1}{2}x[s(x)-\bar{s}(x)]$ (open circles). The unphysical nature of the solution is demonstrated by the fact that $\frac{1}{2}x[s(x)-\bar{s}(x)]$ is larger than $\frac{1}{2}x[s(x)+\bar{s}(x)]$. We also solved the equations using the values $\alpha=0.83$ and $\alpha'=1$ which corresponds to using a subsample of the di-muon data containing only neutrino events. In this case, even the *sum* of the strange and antistrange distributions is negative. This is shown in Fig. 6.

Thus, our analysis strongly suggests that the remaining discrepancy between $F_2^{CCFR}(x,Q^2)$ and $F_2^{NMC}(x,Q^2)$ cannot be completely attributed to differences between the strange and antistrange quark distributions. In other words, assuming parton charge symmetry the two experiments are incompat-

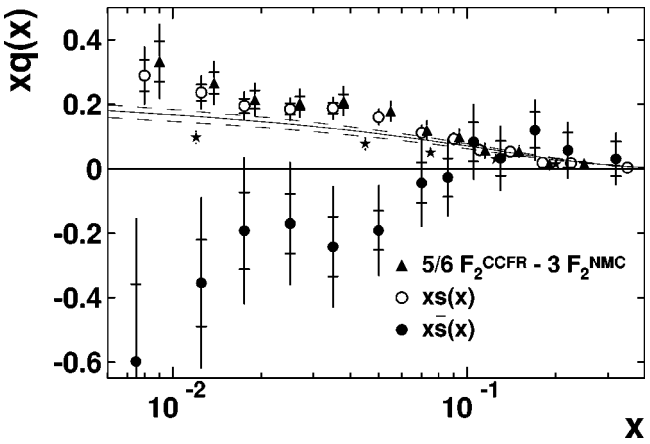

FIG. 4. The strange quark distribution $xs(x)$ (open circles) and antistrange distribution $x\overline{s}(x)$ (solid circles) extracted from the CCFR and NMC structure functions. The difference between the CCFR neutrino and NMC muon structure functions $\frac{5}{6}F_2^{CCFR} - 3F_2^{NMC}$ [see Eq. (15)] is shown as solid triangles. The strange quark distribution extracted by CCFR in a LO analysis [31] is shown as solid stars, while that from a NLO analysis [26] is represented by the solid line, with a band indicating $\pm 1\sigma$ uncertainty in the distribution. (Inner error band: statistical. Outer error band: statistical and systematic added in quadrature.)

ible with each other, even if the antistrange quark distribution is allowed to be different from the strange distribution. (Note, that absolutely *no* restrictions were placed on the antistrange quark distribution, aside from the condition that since it represents a probability density, it must be nonnegative.) We stress that our conclusion is quite different from that of Brodsky and Ma [33], who suggested that allowing $s(x) \neq \overline{s}(x)$ could account for the difference between the two determinations of the strange quark distribution. However, they treated the CCFR structure functions as an average between the neutrino and the antineutrino structure

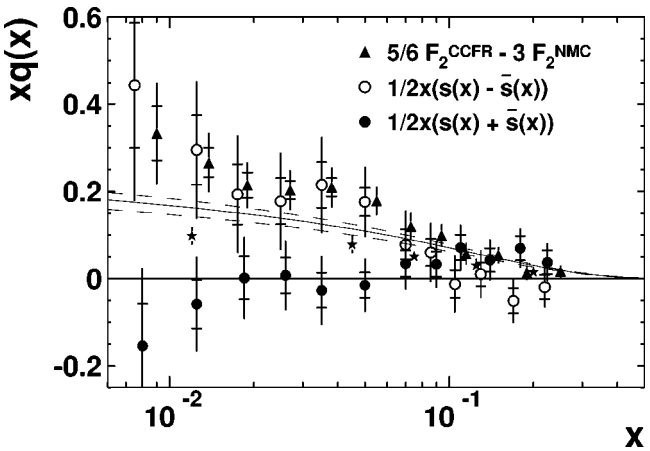

FIG. 5. $\frac{1}{2}x[s(x)+\overline{s}(x)]$ (solid circles) and $\frac{1}{2}x[s(x)-\overline{s}(x)]$ (open circles) as extracted from the CCFR and NMC structure functions and from the dimuon production data. See Fig. 4 for the definition of the other quantities. The strange quark distribution extracted by the CCFR Collaboration is shown as a solid line with a band indicating $\pm 1\sigma$ uncertainty.

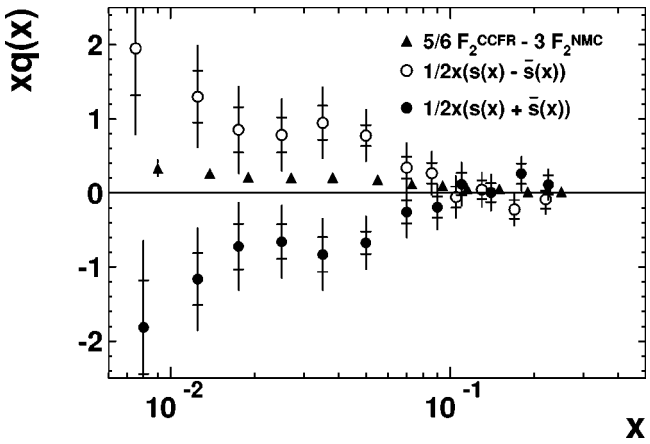

FIG. 6. $\frac{1}{2}x[s(x)+\overline{s}(x)]$ (solid circles) and $\frac{1}{2}x[s(x)-\overline{s}(x)]$ (open circles) as extracted from the CCFR and NMC structure functions and from the dimuon production data using $\alpha' = 1$.

function which corresponds to setting $\alpha = 0.5$.

At this point there are two possibilities to explain the low-x discrepancy observed between the CCFR neutrino and the NMC muon structure functions. Either one of the experimental structure functions (or the strange quark distributions) is incorrect at low x, or parton charge symmetry is violated in this region, since we have shown that neither neutrino shadowing corrections nor an inequality between strange and antistrange quark distributions can explain this experimental anomaly. If we include the possibility of parton CSV, then we can combine the dimuon data for the strange quark distribution, Eq. (16), with the relation between neutrino and muon structure functions, Eq. (15), to obtain the relation

$$\begin{aligned}\frac{5}{6}F_2^{CCFR}(x,Q^2) - 3F_2^{NMC}(x,Q^2) - xs^{\mu\mu}(x) &= \frac{(2\alpha-1)x}{3}[s(x)-\overline{s}(x)] + \frac{(3-5\beta)x}{12}[\delta d(x)+\delta\overline{d}(x)] \\ &\quad - \frac{(3+5\beta)x}{12}[\delta u(x)+\delta\overline{u}(x)] \\ &\quad - \frac{5(1+\beta)(2\alpha-1)x}{12}[\delta u_v(x)-\delta d_v(x)]. \end{aligned} \tag{18}$$

In Eq. (18) we have used the experimental value $\alpha = \alpha'$, and we have defined the valence quark CSV terms $\delta q_v(x) \equiv \delta q(x) - \delta\overline{q}(x)$. We have neglected the effects of possible CSV on the extraction of $s(x)$ from the dimuon data, or on the identification of the structure functions from the neutrino data. This will be discussed below. Since the discrepancy between CCFR and NMC data lies primarily in the very small x-region, where the valence quark distribution is much smaller than the sea quark, the charge symmetry violation should be predominantly in the sea quark distributions. If we set $\delta q_v(x) \approx 0$ in this region, Eq. (18) can be written as

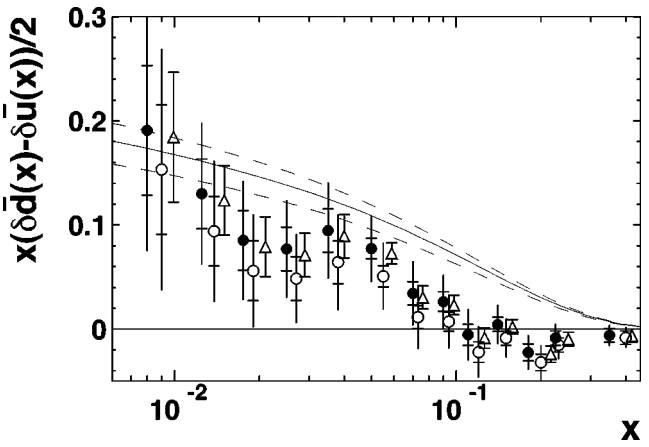

FIG. 7. Charge symmetry violating distributions $x(\delta\bar{d}(x) - \delta\bar{u}(x))/2$ extracted from the CCFR and NMC structure function data and the CCFR dimuon production data under the assumption that $s(x)=\bar{s}(x)$ (solid circles) and $\bar{s}(x)\approx 0$ (open circles) for $\alpha' = 0.83$, and $s(x)=\bar{s}(x)$ (solid circles) and $\bar{s}(x)\approx 0$ (open triangles) for $\alpha'=1$. (For the latter only statistical errors are shown.) $xs(x)$ at $Q^2=4$ GeV^2 obtained by the CCFR Collaboration in a NLO analysis [26] is shown for comparison (solid curve, with 1σ error band).

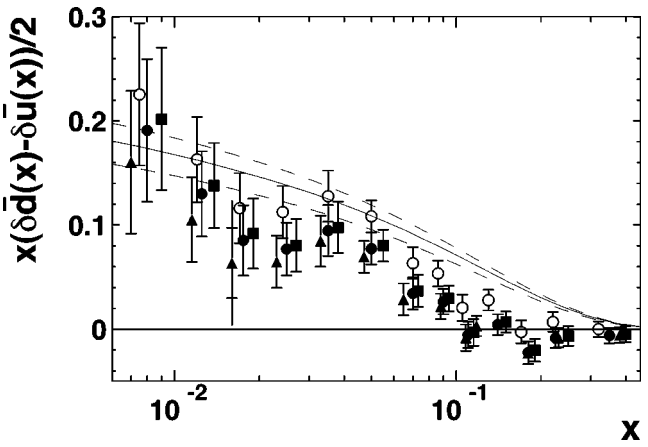

FIG. 8. Uncertainty in the extracted parton CSV term $x(\delta\bar{d}(x) - \delta\bar{u}(x))/2$ due to the parametrization used for the dimuon data on charge symmetry violation. Open circles: LO CCFR distribution; solid circles: CTEQ4L parton distribution [35]; solid rectangles: CTEQ4D parton distribution; solid triangles: NLO CCFR distribution. Here, except for the most ''critical'' point, only statistical errors are shown.

$$\frac{5}{6}F_2^{CCFR}(x,Q^2) - 3F_2^{NMC}(x,Q^2) - xs^{\mu\mu}(x)$$
$$\approx \frac{(2\alpha-1)x}{3}[s(x)-\bar{s}(x)] + \frac{x}{2}[\delta\bar{d}(x)-\delta\bar{u}(x)]$$
$$- \frac{5\beta x}{6}[\delta\bar{d}(x)+\delta\bar{u}(x)]. \quad (19)$$

Since $\beta\approx 0.06$ is quite small, CSV arising from the non-isoscalar nature of the iron target can be neglected, so in the following we neglect the last term of Eq. (19).

Using the experimental data we find that the left hand side of Eq. (19) is positive. Consequently, the smallest value for charge symmetry violation will be obtained if we set $\bar{s}(x) = 0$ [34]. In Fig. 7 we show the magnitude of charge symmetry violation needed to satisfy the experimental values in Eq. (19). The open circles are obtained if we set $\bar{s}(x)=0$, and the solid circles result from setting $\bar{s}(x)=s(x)$. If we use only the neutrino induced di-muon events (i.e. we set $\alpha' = 1$), the coefficient of $x[s(x)-\bar{s}(x)]$, $(5\alpha-3\alpha'-1)/3$, is still positive but smaller in magnitude. Consequently, the influence of the uncertainty in $\bar{s}(x)$ on the extracted CSV is smaller. This is shown as open triangles in Fig. 7.

In obtaining these results, both the structure functions and the strange quark distribution have been integrated over the overlapping kinematic regions, F_2^{CCFR} has been corrected for shadowing effects using the two phase model and we used the CTEQ4L parametrization for $s^{\mu\mu}$ [35]. In Fig. 8 we show the sensitivity of extracted CSV to the parametrization used for $s^{\mu\mu}$. The uncertainty due to different parametrizations has been partly taken into account since the calculated errors already include the uncertainty of the dimuon measurement and most of the parametrizations lie within the experimental errors of the dimuon data [except for LO-CCFR $s(x)$]. We note that the magnitude of the observed charge symmetry violation in the sea quark distributions is independent of whether we use a pure neutrino or antineutrino structure function or a linear combination of neutrino and antineutrino structure functions. This is quite different from strange and antistrange quark effects which are sensitive to the relative weighting of neutrino and antineutrino events in the data sample. Thus, effects due to CSV are independent of the precise value of the relative neutrino flux, α.

The CSV effect required to account for the NMC-CCFR discrepancy is extraordinarily large. It is roughly the same size as the strange quark distribution at small x (compare the open circles in Fig. 7 with the solid line in Fig. 7). The charge symmetry violation necessary to provide agreement with the experimental data is about 25% of the light sea quark distributions for $x<0.1$. The level of CSV required is two to three orders of magnitude larger than the theoretical estimates of charge symmetry violation [36–39]. Note that, if $\bar{s}(x)<s(x)$ in this region, as suggested in Ref. [33], we would need an even larger CSV to account for the CCFR-NMC discrepancy.

Theoretical calculations suggest that $\delta\bar{d}(x)\approx -\delta\bar{u}(x)$ [36,37]. Since those calculations predict a much smaller CSV this conclusion is not very compelling. However, since charge symmetry violation seems to be surprisingly large, it is reasonable to assume that these distributions have opposite signs and reinforce each other. We note that with this sign CSV effects also require large flavor symmetry violation. One might ask whether such large CSV effects would be seen in other experiments. For example, CSV in the nucleon sea could contribute to the observed violation of the Gottfried sum rule [8,37,36] and could explain the Fermilab Drell-Yan experiment [8]. This will be discussed in Sec. IV.

Clearly, CSV effects of this magnitude need further experimental verification. The NuTeV-experiment at Fermilab [40] is able to operate either with pure neutrino or pure antineutrino beams. The extracted structure functions can be used to build different linear combinations, proportional to various combinations of the $\delta\bar{q}$'s and $s\text{-}\bar{s}$. This will be useful to separate CSV from $s\text{-}\bar{s}$ effects.

At small x, our results can be summarized by

$$\delta\bar{d}(x)-\delta\bar{u}(x)\approx\frac{1}{2}(s(x)+\bar{s}(x))\approx\frac{1}{2}\left(\frac{\bar{u}(x)+\bar{d}(x)}{2}\right)$$

$$\delta\bar{d}(x)+\delta\bar{u}(x)\approx 0. \tag{20}$$

From Eq. (2) we note that such a CSV effect would have little or no effect on the F_2 structure functions of isoscalar targets, for either neutrinos or antineutrinos. The major effect for isoscalar targets would be a significant positive contribution to $F_3^{\nu N_0}(x,Q^2)$ at small x, and an equally large negative contribution to $F_3^{\bar{\nu}N_0}(x,Q^2)$.

However, if CSV effects of this magnitude are really present at small x, then we should include charge symmetry violating amplitudes in parton phenomenology from the outset, and re-analyze the extraction of all parton distributions. Given the experimental values $\kappa=2S/(U+D)\approx 0.5$, where S, U and D are the probabilities for strange, up and down quarks averaged over x, and the size of CSV effects suggested by the preceding analysis, we would predict that at small x, $\bar{d}^n(x)\approx 1.25\bar{u}^p(x)$ and $\bar{u}^n(x)\approx 0.75\bar{d}^p(x)$.

IV. EFFECTS OF PARTON CSV ON OTHER OBSERVABLES

If there is substantial CSV, it should also effect other observables. In the following we review the effects which such large CSV terms might have on three quantities; first, the recent search for parton ''flavor symmetry violation'' [FSV] by the Fermilab Drell-Yan experiment E866; second, the extraction of the strange quark distribution; and third, experimental determination of the Weinberg angle $\sin^2(\theta_W)$.

A. Flavor symmetry violation in the proton sea

The results of the recent Fermilab Drell-Yan experiment [7] and the comparison of the proton and neutron structure functions measured by the NMC Collaboration [4] indicate substantial flavor symmetry violation. However, both experimental observations could be attributed to charge symmetry violation, as pointed out by Ma [8] (see also [9]). Furthermore, both CSV and FSV could be present, as suggested by our analysis of the CCFR-NMC discrepancy. Therefore, it is important to examine the effects of CSV on the interpretation of the Fermilab and NMC experiments.

First, we discuss the Drell-Yan experiment which measures the ratio of the dimuon cross sections from proton-deuteron and proton-proton scattering. Since CSV is significant in the small x region, it is a reasonable first approximation to keep only the contributions to the Drell-Yan cross sections which come from the annihilation of quarks of the projectile and antiquarks of the target [41]. In this approximation, the ratio $R\equiv\sigma^{pD}/(2\sigma^{pp})$ is given by

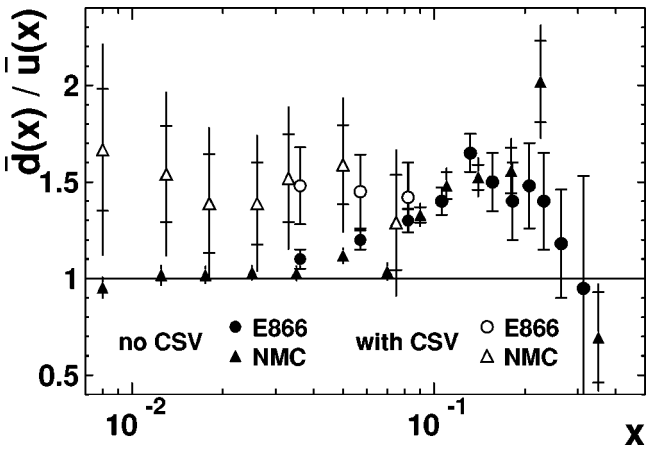

FIG. 9. Solid circles: the ratio $\bar{d}(x)/\bar{u}(x)$ vs x, extracted from the Drell-Yan data of FNAL experiment E866 [7] assuming the validity of charge symmetry. If CS is violated this ratio corresponds to $(\bar{d}(x)-\delta\bar{d}(x))/\bar{u}(x)$. The result obtained by correcting for CSV is shown as open circles. The ratio $\bar{d}(x)/\bar{u}(x)$ extracted from the difference of proton and deuteron structure functions measured by the NMC group [4] is shown as solid and open triangles, without and with CSV, respectively.

$$\frac{\sigma^{pD}}{2\sigma^{pp}}\approx\frac{\left[1+\dfrac{\bar{d}_2}{\bar{u}_2}-\dfrac{\delta\bar{d}_2}{\bar{u}_2}\right]+\dfrac{R_1}{4}\left[1+\dfrac{\bar{d}_2}{\bar{u}_2}-\dfrac{\delta\bar{u}_2}{\bar{u}_2}\right]}{2\left(1+\dfrac{R_1}{4}\dfrac{\bar{d}_2}{\bar{u}_2}\right)}. \tag{21}$$

Here, we introduced the notation $q_j\equiv q(x_j)$ for the quark distributions (x_1 is the projectile x value and x_2 refers to the target), and $R_1\equiv d_1/u_1$.

For large x_F, which corresponds to large x_1, the quantity R_1 is small; if we ignore it, we have the approximate result

$$R=\frac{\sigma^{pD}}{2\sigma^{pp}}\approx\frac{1}{2}\left\{1+\frac{(\bar{d}_2-\delta\bar{d}_2)}{\bar{u}_2}\right\}. \tag{22}$$

If charge symmetry is valid and $\bar{d}_2=\bar{u}_2$, then we would have $R=1$. The experimental values give $R>1$ at small x_2; from Eq. (22), this could be satisfied if either $\bar{d}_2>\bar{u}_2$ or $\delta\bar{d}_2$ was large and negative. However, the value of $\delta\bar{d}(x)$ extracted from the existing neutrino and muon experiments, as discussed in the preceding section, was large and positive at small x. The enhancement is on the order of 25% in the small x region where CSV could be important.

In Fig. 9 the solid circles show the ratio $\bar{d}(x)/\bar{u}(x)$ extracted from the Drell-Yan experiment if we assume the validity of charge symmetry. The open circles in Fig. 9 show the result for $\bar{d}(x)/\bar{u}(x)$ if we include the CSV term which was extracted from the CCFR-NMC data (this is shown in Fig. 7). Inclusion of parton charge symmetry violation sug-

gested by the CCFR-NMC discrepancy plays an important role in the extraction of the FSV ratio $\overline{d}/\overline{u}$, in the region $x<0.1$. The flavor symmetry violation in the sea has to be substantially larger to overcome the CSV term which goes in the opposite direction. In particular, the ratio $\overline{d}(x)/\overline{u}(x)$ does not approach 1 for small x values.

We can invert the extracted ratio to obtain the difference $[(\overline{d}-\delta\overline{d})-\overline{u}]$

$$(\overline{d}-\delta\overline{d})-\overline{u}=\frac{(\overline{d}-\delta\overline{d})/\overline{u}-1}{(\overline{d}-\delta\overline{d})/\overline{u}+1}[(\overline{d}-\delta\overline{d})+\overline{u}]. \quad (23)$$

As a rough approximation, we could neglect $\delta\overline{d}$ in the sum on the right hand side of Eq. (23) and keep it in the difference between $\overline{d}$ and $\overline{u}$ on the left hand side. For $\overline{u}+\overline{d}$ one could use a parametrization. This is exactly the way that $\overline{d}-\overline{u}$ has been extracted from the Drell-Yan data, so that in fact the extracted quantity corresponds to $(\overline{d}-\delta\overline{d})-\overline{u}$ if CSV is present.

The difference, $\overline{d}-\overline{u}$, can also be extracted from the difference between the proton and neutron structure functions measured by the NMC Collaboration [4] using muon deep inelastic scattering. In this case we have

$$\frac{1}{2}(u_v(x)-d_v(x))-\frac{3}{2x}(F_2^p(x)-F_2^n(x))$$
$$=(\overline{d}(x)-\overline{u}(x))-\frac{2}{3}(\delta d(x)+\delta\overline{d}(x))$$
$$-\frac{1}{6}(\delta u(x)+\delta\overline{u}(x)). \quad (24)$$

We can make the approximations $\delta q(x)\approx\delta\overline{q}(x)$ and $\delta\overline{d}(x)\approx-\delta\overline{u}(x)$ (the latter may not be a good approximation since we have FSV), and obtain

$$\frac{1}{2}(u_v(x)-d_v(x))-\frac{3}{2x}(F_2^p(x)-F_2^n)(x)$$
$$\approx[(\overline{d}(x)-\delta\overline{d}(x))-\overline{u}(x)]. \quad (25)$$

Comparing this with Eq. (23) we see that, in a first approximation, the quantities extracted from the two experiments are the same even if both CSV and FSV are present. However, if CSV is present, the term $\delta\overline{d}$ has to be subtracted from the measured quantity to obtain the difference $\overline{d}-\overline{u}$.

We inverted Eq. (25) by dividing both sides by $\overline{d}-\delta\overline{d}+\overline{u}\equiv\overline{u}(r_2+1)$, approximating $\overline{d}-\delta\overline{d}+\overline{u}$ on the left hand side of Eq. (25) by a parametrization of $\overline{d}+\overline{u}$ and solving for $r_2=\overline{d}(x_2)/\overline{u}(x_2)$. The structure functions and the parton distribution are integrated for each data point over the same Q^2 regions as in the analysis of the charge ratio. The result is shown in Fig. 9 as solid triangles. If we subtract the contribution of CSV from the ratio r_2 we obtain the result shown as open triangles in Fig. 9. We see that charge symmetry violation, as suggested by the CCFR-NMC discrepancy, considerably enhances the FSV ratio $\overline{d}/\overline{u}$ in the region $x<0.1$.

It is interesting to investigate the influence of CSV on the Gottfried sum rule. If both CSV and FSV are present the Gottfried sum rule can be expressed as

$$S_G=\frac{1}{3}-\frac{2}{3}\int_0^1 dx[\overline{d}(x)-\overline{u}(x)]+\frac{2}{9}\int_0^1 dx[4\,\delta\overline{d}(x)+\delta\overline{u}(x)]. \quad (26)$$

Now, if $\delta\overline{d}(x)\approx-\delta\overline{u}(x)$ we have

$$S_G=\frac{1}{3}-\frac{2}{3}\int_0^1 dx\{[\overline{d}(x)-\delta\overline{d}(x)]-\overline{u}(x)\}, \quad (27)$$

so that, although the CSV suggested by the CCFR experiment does influence the magnitude of the extracted FSV, it does not change the experimental value of the Gottfried sum rule since the extracted quantities appear in exactly the same form in the Gottfried sum rule as in the Drell-Yan and NMC experiments.

B. Extraction of strange quark distributions

The differential cross section for the production of opposite-sign dimuons, for neutrino and antineutrino deep inelastic scattering from an isoscalar target, are proportional to the quark distributions, the CKM-matrix elements, the fragmentation function $D(z)$ of the struck quark and the weighted average of the semi-leptonic branching ratios of the charmed hadrons B_c

$$\frac{d\sigma(\nu N_0\to\mu^-\mu^+X)}{d\xi\,dy\,dz}\sim\{[u(\xi)+d(\xi)-\delta u(\xi)]|V_{cd}|^2+2s(\xi)|V_{cs}|^2\}D(z)B_c(c\to\mu^+X). \quad (28)$$

For antineutrino scattering the quark distributions should be replaced by the corresponding antiquark distributions. In this equation, ξ is the rescaling variable defined by $\xi=x(1+m_c^2/Q^2)$, with m_c the mass of the produced charm quark. The CCFR Collaboration used this expression together with the parametrization of the quark distributions extracted from their structure function data to determine the strange quark distributions. The strange quark component of the quark sea was allowed to have a different magnitude and shape from the non-strange component. These two degrees of freedom were parametrized by two free parameters κ and α, respectively. Further, they treated B_c and the mass of the charm quark, m_c, as free parameters and performed a χ^2 minimization to find the four free parameters by fitting to distributions of the measured number densities. We note first, that, provided $\delta\overline{u}=-\delta\overline{d}$ [see Eqs. (2) and (20)], charge symmetry violation does not effect the extraction of the non-strange parton distributions from the structure function data for small x-values. For an isoscalar target, these distributions can be determined quite accurately, even if charge symmetry is broken in the manner given by Eq. (20). However, in extracting the strange quark distribution, charge symmetry violation plays an important role. The distribution extracted by the CCFR Collaboration is *not* the strange quark distribution, but

a linear combination of the true strange quark distribution and the term in Eq. (28) coming from CSV. Hence, the distribution measured in the experiment, $s^{CCFR}(x)$, is related to the ''true'' strange quark distribution $s(x)$ by

$$s(x)=s^{CCFR}(x)+\frac{1}{2}\frac{|V_{cd}|^2}{|V_{cs}|^2}\delta\bar{u}(x). \tag{29}$$

Since $|V_{cd}|^2/|V_{cs}|^2\approx 0.05$, the error one makes is roughly two percent, if $\delta\bar{u}$ is of the same order of magnitude as $s(x)$, as the experimental data suggest. $\delta\bar{u}(x)$ is negative and hence the true strange quark distribution should be smaller than that determined by CCFR neglecting charge symmetry violation. Note that we have neglected all other contributions of CSV to the extraction of any other parton distributions, and we neglect higher order corrections, which could be sizable [42,43].

C. Determination of $\sin^2(\theta_W)$

It might appear that the precision measurement of $\sin^2(\theta_W)$ from neutrino deep-inelastic scattering, carried out by the CCFR Collaboration [44], rules out the possibility of large CSV in the parton sea distributions. Sather [38] has previously pointed out that the measurement of $\sin^2(\theta_W)$ is sensitive to possible CSV effects in parton distributions.

If charge symmetry is valid the ratio of the differences of neutrino and antineutrino neutral-current and charged-current cross sections is given by the Paschos-Wolfenstein relation [45]

$$R^-\equiv\frac{\sigma_{NC}^{\nu N_0}-\sigma_{NC}^{\bar{\nu}N_0}}{\sigma_{CC}^{\nu N_0}-\sigma_{CC}^{\bar{\nu}N_0}}=\frac{1}{2}-\sin^2(\theta_W). \tag{30}$$

The CCFR Collaboration used this relation to extract $\sin^2(\theta_W)$ and obtained the value $\sin^2(\theta_W)=0.2255\pm 0.0018(\text{stat})\pm 0.0010(\text{syst})$ [44] which is in very good agreement with the standard model prediction of 0.2230 ± 0.0004 based on measured Z, W and top masses [32]. The precision of this result puts strong constraints on CSV in parton distributions. However, since the measurement of $\sin^2(\theta_W)$ based on the Paschos-Wolfenstein relation is only sensitive to CSV in *valence* quark distributions, the substantial charge symmetry violation in sea-quark distributions found in this analysis does not contradict the precision measurement of $\sin^2(\theta_W)$.

This can be seen as follows. The difference between the neutrino and antineutrino charged-current cross sections is proportional to the difference between F_2^ν and $F_2^{\bar{\nu}}$ and to the sum of xF_3^ν and $xF_3^{\bar{\nu}}$. We see that these linear combinations of the structure functions are only sensitive to $\delta q(x)-\delta\bar{q}(x)$, i.e., CSV in *valence* quark distributions [see Eq. (2)].

The neutral-current neutrino cross sections on an isoscalar target, omitting second generation quark contributions, is given by

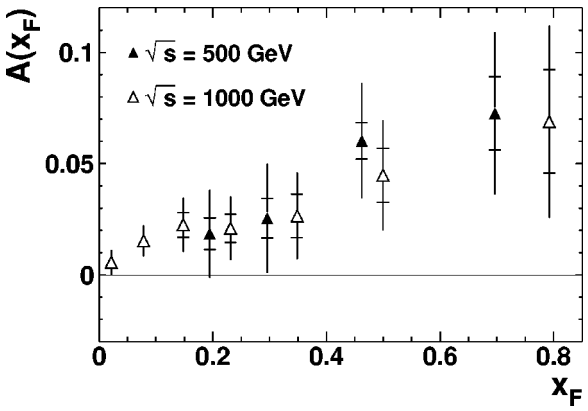

FIG. 10. The forward-backward asymmetry for W production, as defined in Eq. (34). The solid and open triangles are calculated for $\sqrt{s}=500$ GeV and $\sqrt{s}=1000$ GeV, respectively. For $\delta\bar{d}$, the values extracted from the comparison of the NMC and CCFR structure function are used. The errors are the errors of $\delta\bar{d}$ and do not include the errors of the W experiment.

$$\begin{aligned}\frac{d\sigma_{NC}^{\nu N_0}}{dx\,dQ^2}=\frac{G_F^2}{2\pi x}\{&a_u[u(x)+d(x)-\delta d(x)]x\\&+a_d[u(x)+d(x)-\delta u(x)]x\\&+b_u[\bar{u}(x)+\bar{d}(x)-\delta\bar{d}(x)]x\\&+b_d[\bar{u}(x)+\bar{d}(x)-\delta\bar{u}(x)]x\}.\end{aligned} \tag{31}$$

Here, we defined $a_f=l_f^2+r_f^2(1-y)^2$ and $b_f=l_f^2(1-y)^2+r_f^2$ with $f=u,d$ and the couplings of the quarks to the neutral-currents are $l_u=1/2-2/3\sin^2(\theta_W)$, $r_u=-2/3\sin^2(\theta_W)$ and $l_d=-1/2+1/3\sin^2(\theta_W)$, $r_d=1/3\sin^2(\theta_W)$, respectively. The antineutrino cross section can be obtained by interchanging quarks with antiquarks in Eq. (31). We immediately see that the difference between neutrino and antineutrino neutral-current cross sections is only sensitive to CSV in valence quark distributions. Thus the large CSV effects in the nucleon sea quark distributions, suggested by the CCFR-NMC discrepancy, do not influence the measurement of $\sin^2(\theta_W)$ based on the Paschos-Wolfenstein relation.

V. TEST OF PARTON CSV FROM W PRODUCTION AT HADRON COLLIDERS

Clearly, it is important that the charge symmetry violating distributions, $\delta\bar{d}$ and $\delta\bar{u}$, enter with different weights in any observable. Otherwise effects due to CSV are not measurable. In this connection we also note that most of the measured physical observables are proportional to the *sum* rather than the *difference* of the charge symmetry violating quark distributions. However, $\delta\bar{d}$ and $\delta\bar{u}$ are weighted with the charges of the quarks in electromagnetic interactions, such as deep inelastic scattering with charged leptons and Drell-Yan processes. In fact, a comparison between charged lepton and neutrino induced structure functions was necessary to detect

CSV as we have shown in this paper. We also discussed the implications of CSV on the Drell-Yan process. In the following, we show that *W*-boson production in proton deuteron collisions can also be used to test the CSV found in this paper, if we define a suitable observable. Such measurements could be carried out at RHIC and LHC. Vigdor [46] originally suggested that asymmetry in *W*-boson production could be used as a test of parton charge symmetry.

The cross sections for $pD\to W^+X$ and $pD\to W^-X$ are given by

$$\frac{d\sigma}{dx_F}(pD\to W^+X)\sim\{u(x_1)[\bar{u}(x_2)+\bar{d}(x_2)-\delta\bar{u}(x_2)]+\bar{d}(x_1)[u(x_2)+d(x_2)-\delta d(x_2)]\}\cos^2\Theta_c$$
$$+\{u(x_1)\bar{s}(x_2)+\bar{s}(x_1)[u(x_2)+d(x_2)-\delta d(x_2)]\}\sin^2\Theta_c \tag{32}$$

$$\frac{d\sigma}{dx_F}(pD\to W^-X)\sim\{d(x_1)[\bar{u}(x_2)+\bar{d}(x_2)-\delta\bar{d}(x_2)]+\bar{u}(x_1)[u(x_2)+d(x_2)-\delta u(x_2)]\}\cos^2\Theta_c$$
$$+\{\bar{u}(x_1)s(x_2)+s(x_1)[\bar{u}(x_2)+\bar{d}(x_2)-\delta\bar{d}(x_2)]\}\sin^2\Theta_c\,. \tag{33}$$

We note that the Cabibbo favored terms in the sum of the W^+ and W^- cross sections are invariant under the interchange of x_1 and x_2, if charge symmetry is valid. However, the Cabibbo suppressed part of the sum contains terms which are not invariant under $x_1\leftrightarrow x_2$, even if charge symmetry is a good symmetry. Thus, if we define the forward-backward asymmetry as

$$A(x_F)=\frac{\left(\frac{d\sigma}{dx_F}\right)^{W^+}(x_F)+\left(\frac{d\sigma}{dx_F}\right)^{W^-}(x_F)-\left(\frac{d\sigma}{dx_F}\right)^{W^+}(-x_F)-\left(\frac{d\sigma}{dx_F}\right)^{W^-}(-x_F)}{\left(\frac{d\sigma}{dx_F}\right)^{W^+}(x_F)+\left(\frac{d\sigma}{dx_F}\right)^{W^-}(x_F)+\left(\frac{d\sigma}{dx_F}\right)^{W^+}(-x_F)+\left(\frac{d\sigma}{dx_F}\right)^{W^-}(-x_F)}, \tag{34}$$

we see that it will be proportional to charge symmetry violating terms and terms containing strange quarks. Assuming $s(x)=\bar{s}(x)$ the numerator of Eq. (34), $\Delta(d\sigma/dx_F)(x_F)$ is given by

$$\Delta\left(\frac{d\sigma}{dx_F}\right)(x_F)=\{-[u(x_1)\,\delta\bar{u}(x_2)+d(x_1)\,\delta\bar{d}(x_2)+\bar{u}(x_1)\,\delta u(x_2)+\bar{d}(x_1)\,\delta d(x_2)]\cos^2\Theta_c$$
$$+s(x_1)[d(x_2)+\bar{d}(x_2)-\delta d(x_2)-\delta\bar{d}(x_2)]\sin^2\Theta_c\}-(x_1\leftrightarrow x_2). \tag{35}$$

In the following, we use $\delta\bar{u}\approx-\delta\bar{d}$, as suggested by our analysis, and note that as the charge symmetry violating distribution is of the same order of magnitude as the strange quark distribution, terms proportional to $\sin^2\Theta_c$ can be neglected. Further, we make the approximations $\delta\bar{q}(x_2)\approx\delta q(x_2)$ for $x_2\leqslant 0.1$ and $\delta\bar{q}(x_1)\approx 0$ for large x_1. We then obtain

$$\Delta\left(\frac{d\sigma}{dx_F}\right)(x_F)=\{[u(x_1)+\bar{u}(x_1)-d(x_1)-\bar{d}(x_1)]\,\delta\bar{d}(x_2)$$
$$+[\,\delta u(x_1)\bar{u}(x_2)+\delta d(x_1)\bar{d}(x_2)]\}\cos^2\Theta_c\,. \tag{36}$$

For large x_F, the forward-backward asymmetry [due to the first term in Eq. (36)] is proportional to $\delta\bar{d}$ times the difference between the up and down valence quark distributions. The second term is sensitive to CSV in valence quark distributions. However, if $\delta d\approx-\delta u$ for valence quarks, as suggested by theoretical considerations [37], the second term of Eq. (36) is approximately $[\bar{d}(x_2)-\bar{u}(x_2)]\,\delta d(x_1)$ and is only non-zero if we have FSV. Further, if $\delta d(x_1)$ is positive for large x_1, as theoretical calculations suggest [37,38] then the second term will contribute positively to the asymmetry, since $\bar{d}-\bar{u}>0$, so that it would enhance any asymmetry expected on the basis of CSV in the sea quark distributions suggested by the NMC-CCFR data.

We calculated the expected asymmetry $A(x_F)$ for $\sqrt{s}=500$ GeV and $\sqrt{s}=1000$ GeV using the values of $\delta\bar{d}$ extracted in Sec. II. The results are shown in Fig. 10. The error bars represent the errors associated with $\delta\bar{d}$ and do not include the errors of the *W* experiment. In the calculation, we retained all terms in Eq. (33). The result obtained by using

the approximation in Eq. (36) differs only by a few percent from the full calculation. We predict considerable asymmetries for large x_F.

VI. CONCLUSIONS

In conclusion, we have examined in detail the discrepancy at small x between the CCFR neutrino and NMC muon structure functions. Assuming that both the structure functions and strange quark distributions have been accurately determined in this region, we explored the possible reasons for this discrepancy. First, we re-examined the shadowing corrections to neutrino deep inelastic scattering and concluded that shadowing cannot account for more than half of the difference between the CCFR and NMC structure functions. Next, we compared two determinations of the strange quark distributions: the ''direct'' method, obtained by measuring opposite sign dimuon production from neutrino and antineutrino reactions, and by comparing the CCFR and NMC structure functions. The strange quark distributions extracted by these two methods are incompatible with each other, even if we allow the antistrange quark distribution to differ from the strange distribution in an unconstrained fashion.

The only way we can make these data compatible is by assuming charge symmetry violation in the sea quark distributions. The CSV amplitudes necessary to obtain agreement with experiment are extremely large—they are of the same order of magnitude as the strange quark distributions, or roughly 25% the size of the nonstrange sea quark distributions at small x. Such CSV contributions are surprisingly large: at least two orders of magnitude greater than theoretical predictions of charge symmetry violation. We discussed their influence on other observables, such as the FSV ratio measured recently in a proton deuteron Drell-Yan experiment, on the Gottfried sum rule and on the experimental determination of the Weinberg angle $\sin^2\theta_W$. We showed that such large CSV effects could be tested by measuring asymmetries in W boson production at hadron colliders such as RHIC or LHC. Such experiments could detect sea quark CSV effects, if they were really as large as is suggested by current experiments.

ACKNOWLEDGMENTS

This work was supported in part by the Australian Research Council. One of the authors (J.T.L.) was supported in part by the National Science Foundation research contract PHY-9722706. J.T.L. wishes to thank the Special Research Center for the Subatomic Structure of Matter for its hospitality during the period when this research was carried out.

[1] G. A. Miller, B. M. K. Nefkens, and I. Slaus, Phys. Rep. **194**, 1 (1990).
[2] E. M. Henley and G. A. Miller, in *Mesons in Nuclei*, edited by M. Rho and D. H. Wilkinson (North-Holland, Amsterdam, 1979).
[3] J. T. Londergan and A. W. Thomas, in *Progress in Particle and Nuclear Physics*, edited by A. Faessler (Elsevier Science, Amsterdam, 1998), Vol. 41, p. 49.
[4] NMC Collaboration, P. Amaudruz *et al.*, Phys. Rev. Lett. **66**, 2712 (1991); Phys. Lett. B **295**, 159 (1992).
[5] K. Gottfried, Phys. Rev. Lett. **18**, 1174 (1967).
[6] NA51 Collaboration, A. Baldit *et al.*, Phys. Lett. B **332**, 244 (1994).
[7] E866 Collaboration, E. A. Hawker *et al.*, Phys. Rev. Lett. **80**, 3715 (1998).
[8] B. Q. Ma, Phys. Lett. B **274**, 433 (1992); B. Q. Ma, A. W. Schäfer, and W. Greiner, Phys. Rev. D **47**, 51 (1993).
[9] F. M. Steffens and A. W. Thomas, Phys. Lett. B **389**, 217 (1996).
[10] J. T. Londergan, S. M. Braendler, and A. W. Thomas, Phys. Lett. B **424**, 185 (1998).
[11] J. T. Londergan, Alex Pang, and A. W. Thomas, Phys. Rev. D **54**, 3154 (1996).
[12] NMC Collaboration, M. Arneodo *et al.*, Nucl. Phys. **B483**, 3 (1997).
[13] CCFR Collaboration, W. G. Seligman *et al.*, Phys. Rev. Lett. **79**, 1213 (1997).
[14] C. Boros, J. T. Londergan, and A. W. Thomas, Phys. Rev. Lett. **81**, 4075 (1998).
[15] W. G. Seligman, Ph.D. thesis, Columbia University, 1997.
[16] L. W. Whitlow *et al.*, Phys. Lett. B **250**, 193 (1990).
[17] M. Arneodo, Phys. Rep. **240**, 301 (1994) and the references given therein.
[18] C. Boros, J. T. Londergan, and A. W. Thomas, Phys. Rev. D **58**, 114030 (1998).
[19] J. Kwiecinski and B. Badelek, Phys. Lett. B **208**, 508 (1988); Rev. Mod. Phys. **68**, 445 (1996).
[20] W. Melnitchouk and A. W. Thomas, Phys. Lett. B **317**, 437 (1993); Phys. Rev. C **52**, 3373 (1995).
[21] C. A. Piketty and L. Stodolsky, Nucl. Phys. **B15**, 571 (1970).
[22] T. H. Bauer, R. D. Spital, D. R. Yennie, and F. M. Pipkin, Rev. Mod. Phys. **50**, 261 (1978).
[23] J. S. Bell, Phys. Rev. Lett. **13**, 57 (1964).
[24] B. Z. Kopeliovich and P. Marage, Int. J. Mod. Phys. A **8**, 1513 (1993).
[25] S. L. Adler, Phys. Rev. **135**, B963 (1964).
[26] CCFR Collaboration, A. O. Bazarko *et al.*, Z. Phys. C **65**, 189 (1995).
[27] A. I. Signal and A. W. Thomas, Phys. Lett. B **191**, 205 (1987).
[28] W. Melnitchouk and M. Malheiro, Phys. Rev. C **55**, 431 (1997).
[29] X. Ji and J. Tang, Phys. Lett. B **362**, 182 (1995).
[30] H. Holtmann, A. Szczurek, and J. Speth, Nucl. Phys. **A596**, 631 (1996).
[31] CCFR Collaboration, S. A. Rabinowitz *et al.*, Phys. Rev. Lett. **70**, 134 (1993).
[32] Particle Data Group, L. Montanet *et al.*, Phys. Rev. D **50**, 1173 (1994).
[33] S. J. Brodsky and B. Q. Ma, Phys. Lett. B **381**, 317 (1996).
[34] The assumption $\overline{s}(x)=0$ violates the sum rule constraint of

Eq. (17). We use this unphysical assumption only to illustrate a range of possibilities for the parton CSV contribution.
[35] H. L. Lai *et al.*, Phys. Rev. D **55**, 1280 (1997).
[36] C. J. Benesh and J. T. Londergan, Phys. Rev. C **58**, 1218 (1998).
[37] E. Rodionov, A. W. Thomas, and J. T. Londergan, Mod. Phys. Lett. A **9**, 1799 (1994).
[38] E. Sather, Phys. Lett. B **274**, 433 (1992).
[39] C. J. Benesh and T. Goldman, Phys. Rev. C **55**, 441 (1997).
[40] NuTeV Collaboration, T. Bolton *et al.*, ''Precision Measurements of Neutrino Neutrino Neutral Current Interactions Using a Sign Selected Beam,'' Fermilab Proposal P-815, 1990.
[41] In general, one should retain contributions from antiquarks in the projectile and quarks in the target. However, since the CSV terms we extract seem to be so large, in this case one can neglect these contributions for large Feynman x_F.
[42] V. Barone, M. Genovese, N. N. Nikolaev, E. Predazzi, and B. G. Zahkarov, Phys. Lett. B **317**, 433 (1993); **328**, 143 (1994).
[43] M. Gluck, S. Kretzer, and E. Reya, Phys. Lett. B **380**, 171 (1996); **405**, 391(E) (1997); **398**, 381 (1997).
[44] CCFR Collaboration, K. S. McFarland *et al.*, hep-ex/9806013.
[45] E. A. Paschos and L. Wolfenstein, Phys. Rev. D **7**, 91 (1973).
[46] S. Vigdor, Second International Symposium on Symmetries in Subatomic Physics, Seattle, WA, 1997 (unpublished).